Turkish Journal of Physics

Volume 30 | Number 4 Article 6

1-1-2006

Applications of Genetic Algorithm to Quantum Mechanical Systems

MEHMET ŞAHİN

ÜLFET ATAV

MEHMET TOMAK

Turk J Phys
30 (2006) , 253 – 275.

Applications of Genetic Algorithm to Quantum Mechanical Systems

Mehmet ŞAHİN[1], **Ülfet ATAV**[1], **Mehmet TOMAK**[2]
[1] *Dept. of Physics, Faculty of Sciences and Arts, Selçuk University, Kampus 42031 Konya, TURKEY*
e-mail: sahinm@selcuk.edu.tr

[2] *Dept. of Physics, Middle East Technical University, İnönü Bulvarı 06531 Ankara, TURKEY*

Received 18.07.2006

Abstract

Genetic algorithm (GA) inspired by the biological world is a general search and optimization method. It was first proposed by Holland in 1975. GA has been applied to many scientific areas especially in engineering optimization problems. It is also used in solving of quantum mechanical problems. In this study, we have applied this method to different realistic quantum mechanical problems of both self-consistent and non-self-consistent type. The results obtained are compared with the results of other methods and it is seen that the GA can be a very powerful alternative to some other traditional techniques such as variational method.

Key Words: genetic algorithm, quantum dot, heterojunction.

1. Introduction

The recent developments in the fabrication technology have given an opportunity to confine the electrons in two-, one- and zero-dimensional semiconductor structures [1, 2]. Semiconductor quantum nanostructures (quantum wells, wires or dots) have found various application areas especially as electronic devices such as single electron transistor, quantum well and quantum dot infrared photo detector (QWIP and QDIP) [3, 4, 5]. Therefore, these structures have been intensively studied both theoretically and experimentally in condensed matter physics [5, 6, 7]. Many analytical and numerical studies on energy levels and other physical properties of quantum dots (QDs) have been reported [6–10]. Different techniques and approximations had been used in these studies including variational method, perturbation method, matrix diagonalization, Monte Carlo etc. Each one of these techniques has their own advantages and disadvantages.

For example, the traditional variational method has the advantage of being simple and straightforward, hence, it is one of the most frequently used techniques. However, the chosen trial wave function must be well suited for describing the system under consideration. If the wave function is not properly chosen, the results may be far from the exact ones.

In addition to these techniques, recently, an optimization method, namely the genetic algorithm, has begun to be used in computations of the electronic structures [11, 12, 13]. Genetic algorithm (GA) has been applied to many scientific areas and engineering optimization and improvement problems since it was proposed by Holland [14]. Bennett and Shapiro [15] have applied the GA to the ground states of simple random Ising-spin systems. Kim et al. [16] have presented a parameter optimization technique for

GaAs/AlGaAs multiple quantum well avalanche photodiodes by GA. Chaudbury and Bhattacharyya [17], and Nakanishi and Sugawara [18] have numerically solved the Schrödinger equation by GA. Grigorenko and Garcia have used this method to calculate the ground state of one and two particle quantum systems [19, 20], also, they performed a calculation of the partition function using quantum GA [21]. A new approach for solving the Schrödinger equation based on GA and artificial neural network (ANN) has been presented by Sugawara [22]. Chakraborti et al. [23] have used GA to determine the ground state structures of a number of Si-H clusters. Şahin et al. [24] have applied it to the determination of mass transfer coefficients in crystal growth. GA was applied to a non-linear fitting problem by Brunetti [25]. Liu et al. [26] have used evolutionary algorithm to calculate the ground state energy of double-electron atoms. Erkoç et al. [27] have applied it to geometry optimization of microclusters.

The quantum mechanical application of GA, is usually called quantum genetic algorithm (QGA) and is generally limited only to textbook problems [17, 19, 20, 22, 28]. QGA involves the minimization of the total energy just like in conventional variational method but, it has a probabilistic nature. When it is used in wave function optimization, the wave function in the QGA is not constrained by a prescribed analytical form and it gives results much better than conventional variational method. Application of QGA is not complicated, and it can be applied to any problem stated on a variational basis. The choice of the initial population is not very important, the system under consideration need not be represented very well by the initial population. Especially, after a few tens of generations, the method converges to a wave function, which quite satisfactorily describes the system under consideration. This fast initial convergence of the method is used in some hybrid methods [29] for the determination of sufficiently good initial guesses. However, starting out with a population describing the system very well, of course, decreases the time required for the convergence.

In this study, the application areas of this method have been extended to realistic quantum mechanical systems. For this purpose, we have taken into consideration different low dimensional systems, e.g. hydrogenic donor impurity in a spherical quantum dot, modulation doped heterojunction and many-electron quantum dot.

The main purpose of this study is to extend the application area of genetic algorithm in to the analysis of quantum mechanical problems and to evaluate the effect of some details on the efficiency of the method.

2. Details of Genetic Algorithm

In spite of the fact that quantum mechanical applications of GA method is based essentially on energy minimization as other variational procedures, it exhibits some important differences. These differences can be summarized as follows: (i) GA employs the coding of any parameter (or parameter set), not parameters themselves, (ii) it starts from any initial population of possible solution, not from a single value or analytical expression, (iii) it uses some fitness (or objective) information in procedure, not any derivative or auxiliary knowledge, and (iv) it follows the probabilistic rules, instead of the deterministic ones. (v) in the QGA method all the parameters can be changed simultaneously, so that a faster convergence can be obtained especially for the variational problems with many parameters [30, 31].

There are two main variants of the quantum mechanical application of GA: first, parameter optimization and the second wave function optimization. Let $\phi(\alpha_1, \alpha_2,..., \alpha_n)$ be a trial wave function with the parameters α_i for a parameter optimization problem, then the initial population is formed by choosing random values of the parameters α_i. These parameters are then substituted into the analytical expression of the trial wave function. Each set of parameters is called an individual, and the total number of individuals is named as the population size. If the QGA is to be used for wave function optimization then the wave function is discretized on a mesh, and the numerical values of these wave functions at the mesh points makes up an individual. An analytical expression and some set of randomly chosen parameters,α_i, might be used for setting up the initial population. However all subsequent calculations are performed over the values of the wave functions at the mesh points. Therefore, the solution is not restricted by the analytical form used to set up the initial population.

Each wave function (individual) in this initial population is normalized by the relation

$$\phi_n = A_n \tilde{\phi}_n, \tag{1}$$

where ϕ_n and $\tilde{\phi}_n$ are the normalized and unnormalized wave functions respectively. The normalization constant of the individual, A_n, is obtained from,

$$\langle \phi_n | \phi_n \rangle = A_n^2 \left\langle \tilde{\phi}_n \middle| \tilde{\phi}_n \right\rangle = A_n^2 \int \tilde{\phi}_n^* \tilde{\phi}_n d^3r = 1. \tag{2}$$

For each individual (wave function) in this population the expectation value of the energy is determined from

$$E_n[\phi] = \left\langle \phi_n \middle| \hat{H} \middle| \phi_n \right\rangle = \int \phi_n^* \hat{H} \phi_n d^3r. \tag{3}$$

Here, the index n identifies the individual. QGA starts out with a population of possible solutions of the problem under consideration and then proceeds with three basic operations: i) copying or reproduction, ii) crossover, iii) mutation. A probability of occurrence is chosen for each one of these operations. In practice, generally, a high crossover probability is chosen so that the variety in the population is increased. On the other hand, the mutation probability is chosen to be small. If a high mutation probability is chosen, the convergence slows down and the fluctuations increases. Production of better new generations is the main objective of all the genetic operations. To guide the genetic operations to produce better generations, a fitness value is defined for each individual and the genetic operations are performed according to these fitness values. Fitness value of an individual can be regarded as the probability of survival for that individual (or its genetic code). In most quantum mechanical applications the objective is to reach to the minimum energy, therefore the individuals with lower energy should have higher fitness values and the individuals with higher energy should have lower fitness values. There are many possible choices for evaluation of the fitness values. Inspired by the Boltzmann factor in the statistical mechanics, here we use the following expression for fitness values

$$\mu_i = \frac{\exp\left(-\beta\left(E_i - E_{ort}\right)\right)}{\sum_{i=1}^{N_{pop}} \exp\left(-\beta\left(E_i - E_{ort}\right)\right)}, \qquad (i = 1, 2, 3..., N_{pop}). \tag{4}$$

Here, μ_i is the fitness of the i'th individual, N_{pop} is the size of the population, β is an arbitrary constant, and $E_{ort} = \frac{1}{N_{pop}} \sum E_i$ is the average energy expectation value for the population. It is clear from Eq. (4) that $\sum \mu_i = 1$, so that μ_i can be regarded as probability for the survival of the i'th individual.

2.1. Copying

Following the determination of fitness values for each individual, N_{pop} individuals are drawn from the population to produce the new generation. Each individual have a chance of winning proportional to its fitness value, and one individual can be drawn more than once. Therefore, some individuals may appear more than once in the new generation while some of them do not appear at all. Thus the new generation is dominated by individuals having higher fitness values, however even the individual with smallest fitness value have a chance of surviving. The individuals chosen in this way are used as parents of the new generation, other genetic operations are performed on these chosen individuals.

Different selection schemes can be used for the copy process for example roulette wheel selection, tournament selection, ranking selection etc. [32-35].

2.2. Crossover

The crossover occurring in the nature can be defined as an exchange of genes between two chromosomes. The purpose of this operation is to produce better individuals using the existing ones. In order to do this, two individuals are randomly chosen from the population, then each one of these two individuals are divided into two parts by cutting at a random position, then the parts are interchanged between the individuals. This process is schematically shown in Figure 1.

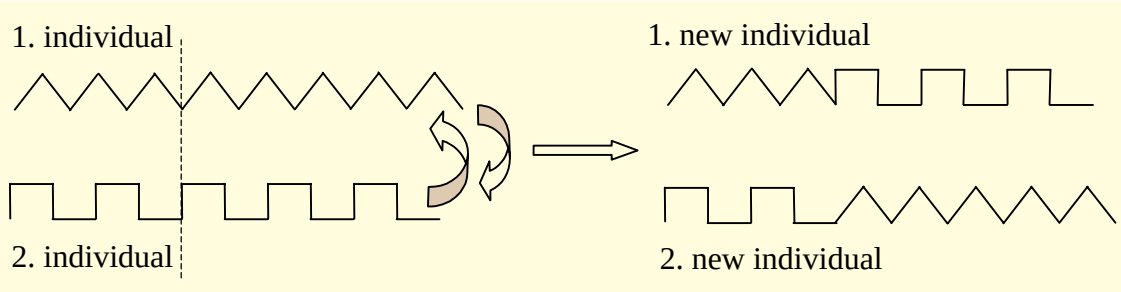

Figure 1. Schematic representation of crossover operation.

In the parameter optimization, the cross over operation is, generally, performed over the binary codes of the numerical values of the parameters. Representations of such a crossover operation with one and two cut points are shown in Figure 2.

It is much easier to work with the numerical values of the wave functions in the wave function optimization. Let us consider, randomly chosen two wave functions $\phi_1(x)$ and $\phi_2(x)$. If we were to obtain two new wave functions by crossing these wave functions, then the new wave functions are defined in terms of the old ones by

$$\begin{aligned} \tilde{\phi}_1'(x) &= \phi_1(x)\, St(x) + \phi_2(x)\,(1 - St(x)) \,, \\ \tilde{\phi}_2'(x) &= \phi_2(x)\, St(x) + \phi_1(x)\,(1 - St(x)) \,, \end{aligned} \tag{5}$$

Note that, in this operation the new wave functions are weighted averages of the older ones, and the function $St(x)$ determines the contribution of each one of the old wave functions. The shape of the function $St(x)$ is very important, it should have a smooth shape because discontinuities or very sharp changes in either the wave functions or in its derivatives are physically unacceptable. In this study we have used the following step function with a smooth transition for the crossover operations [19, 36]

$$St(x) = \frac{1}{2}\left[1 + \tanh\left(\frac{x - x_0}{c^2}\right)\right] \quad . \tag{6}$$

where, x_0 is a random position within the limits of the system, and c is a number determining the sharpness of the step function. Smooth step function $St(x)$ is shown in Figure 3 for three different values of c when $x_0 = 1.0$. It is clear from the figure that the sharpness of the step function increases with decreasing values of c.

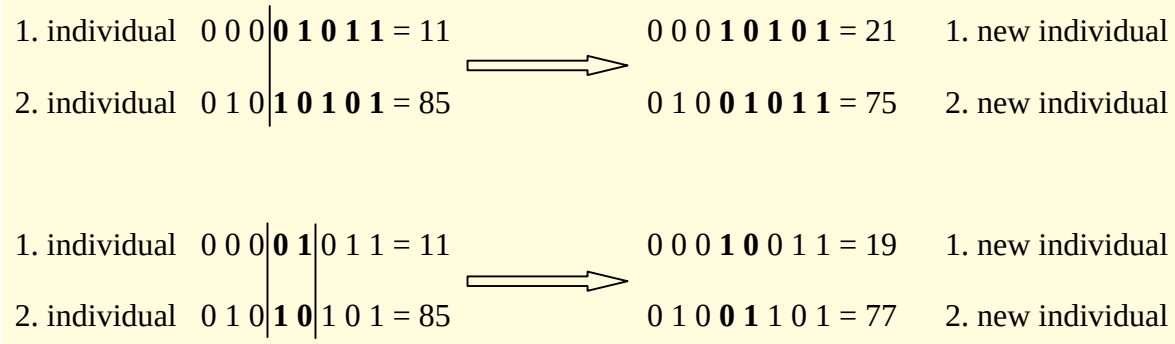

Figure 2. Representation of the single and two points crossover in binary code.

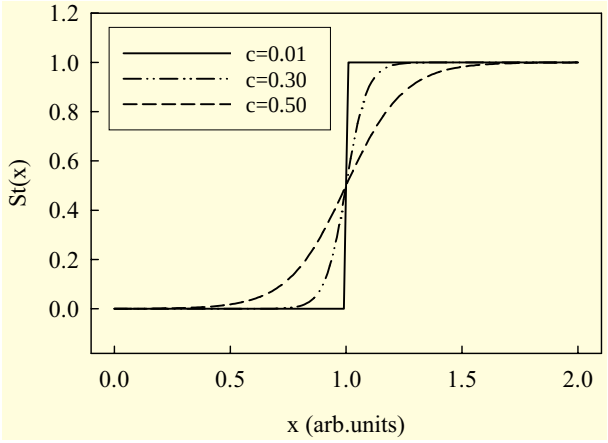

Figure 3. Smooth step function for three different values of c.

Choosing the St function as a constant random value in the range (0,1) is another method for the realization of crossover operation. This kind of cross over would not cause any discontinuities when the original wave functions are smooth.

Two randomly chosen wave functions are shown in Figure 4. New wave functions, obtained from these by a sharp and a smooth step function are shown in Figure 5 a and b respectively. Note that, the new wave functions in Figure 5 a shows a sharp increase or decrease which is physically unacceptable, whereas the wave functions in Figure 5 b displays a smooth behavior.

2.3. Mutation

Sometimes, the search process might fall into local minima, i.e. all the individuals of a generation might be in the valley of the same minima. Such a local minima and a global minima are seen in Figure 6. In this case, it is impossible to get out of this valley with only crossover operations. Mutation operations are used to get away from such local minima. In contrast with the crossover operation, mutation operation is performed on only one individual. When the binary coding is employed, mutation operation corresponds to reversing the value of a bit (chromosome) from 1 to 0 (or from 0 to 1).

Wave function optimization is quite different from the parameter optimizations. Care should be taken in the application of mutation: changing the value of the wave function arbitrarily at one mesh point would result in discontinuities, which are physically unacceptable. A Gaussian distribution can be used as the mutation function to prevent such a situation [19]

$$F_M(x) = A \exp\left(\frac{-(x-x_0)^2}{\delta^2}\right), \tag{7}$$

where, A is the amplitude of the mutation, and δ is an arbitrary number determining the width of the mutation and x_0 is a position within the definition range of the problem. However, δ value should not be very small, otherwise the mutation corresponds to a very sharp spike over the wave function. If we add the mutation function to a randomly chosen wave function we obtain

$$\tilde{\phi}_1'(x) = \phi_1(x) + F_M(x). \tag{8}$$

The solid line in Figure 7 shows a wave function corresponding to the solution of the Schrödinger's equation for an electron in an infinitely deep spherical well. Other two lines shows the cases after the application of mutations with two different amplitudes. Also Figure 8 shows the same wave function after the application of mutations with two different widths. It is clear from both figures that very large amplitudes and very small widths result in physically unacceptable wave functions.

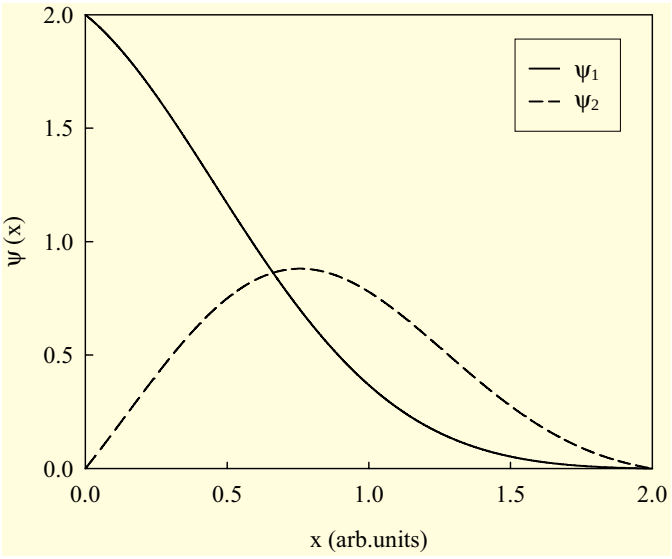

Figure 4. Randomly chosen two wave functions.

Furthermore, constant amplitude mutations are also employed by adding a constant small number to the wave function at every space point. Another approach is to decrease the amplitude of the mutations as the generations go by. Such variable mutation intensity is seen in Eq. (9) [35]

$$\Delta = \left(1 - C^{(1-iter/maxit)^d}\right), \tag{9}$$

where C is a number between 0 and 1, *iter* is the number of current generation, *maxit* is maximum number of generations for the mutation to be applied and d is a parameter to be adjusted. As seen in Figure 9, it is clear that the amplitude of the mutation decreases and it reaches to zero when the number of generation reaches to *maxit*.

All details of the genetic operations (copy, crossover and mutation) can be found in Refs. [11–13, 30–36].

3. Applications of the QGA and the results

In this section, applications of quantum genetic algorithm to different problems are presented. The first application is a hydrogenic impurity problem and the next application is an analysis of a modulation doped heterojunction. The third and the last application is self-consistent determination of the energy level of an N-electron quantum dot.

3.1. Energy Levels of a Hydrogenic Impurity in a Quantum Dot

The Hamiltonian for a spherical quantum dot with an on center hydrogenic impurity for $\ell = 0$ is

$$\hat{H} = -\frac{\hbar^2}{2m}\frac{1}{r^2}\frac{\partial}{\partial r}\left(r^2\frac{\partial}{\partial r}\right) - \frac{e^2}{4\pi\varepsilon_0 r} + V(r) \tag{10}$$

where m is the electronic mass, e is the electronic charge, ε_0 is the electrical permittivity and $V(r)$ is the confining potential defined by

$$V(r) = \begin{cases} 0 & r \le R \\ \infty & r > R \end{cases} . \tag{11}$$

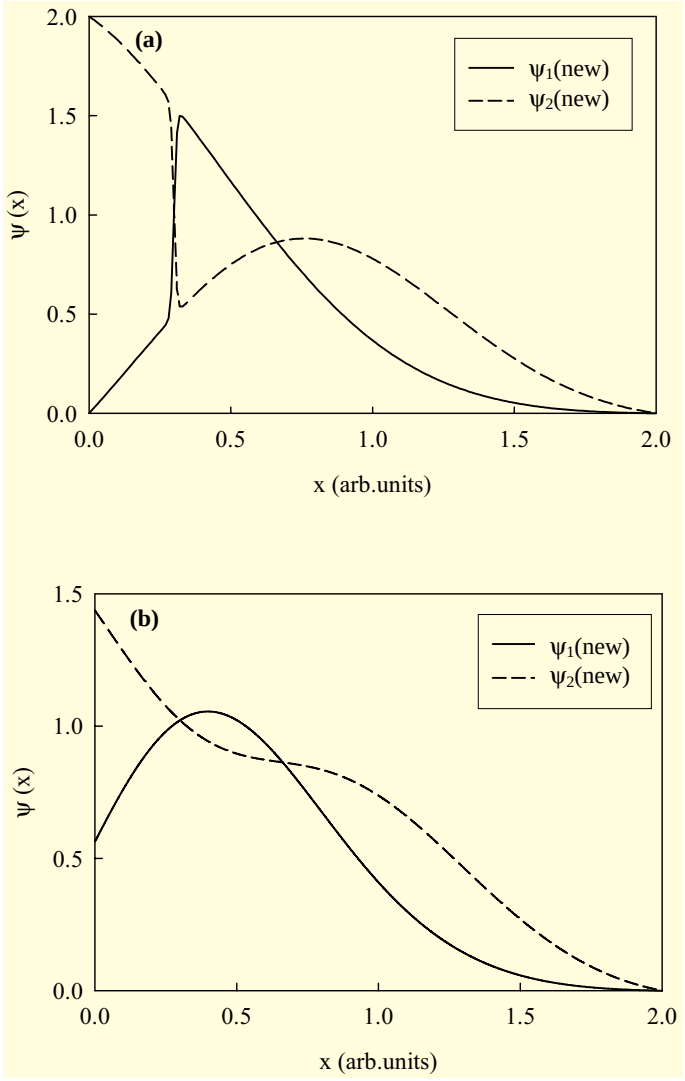

Figure 5. Wave functions after the crossover operation by using the smooth step function. a) for c=0.1, b) for c=0.8

In this study we have considered an infinitely deep quantum dot, therefore, apart from the confining potential the model is equivalent to a hydrogen atom. The problem is to find the energy eigenvalues, E_n, and the corresponding wave functions, ϕ_n, of the Hamiltonian i.e. solving the eigenvalue equation

$$(\hat{H} - E_n)\phi_n = 0, \tag{12}$$

under proper boundary conditions. Our purpose is to compare the QGA with the variational method thus we have chosen such a simple problem where both of the methods can easily be applied. In all our subsequent calculations we have used the atomic units where $m = e = \hbar$=1. The trial wave function for this system is

$$\phi(r) = \begin{cases} A\frac{\sin(kr)}{r}\exp(-\lambda r), & r \le R \\ 0, & r > R \end{cases}, \tag{13}$$

and it satisfies the required boundary conditions [37]. Where, A is the normalization constant, $k = \pi/R$ and λ is the variational parameter. The normalization constant A can be determined for any λ from the relation

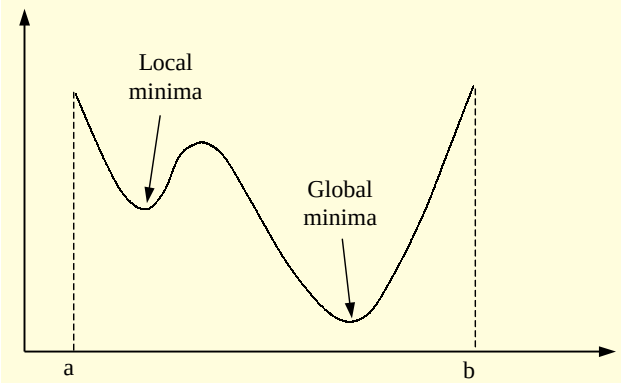

Figure 6. Local and global minima of any function.

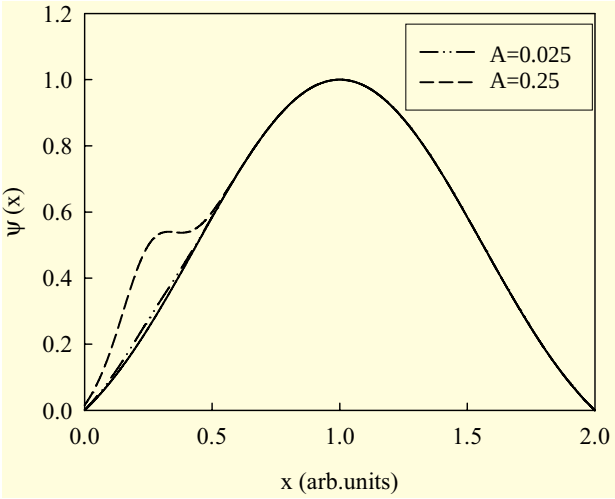

Figure 7. The effect of the mutation amplitude on the wave function.

$$\int \phi^{*}(r)\,\phi(r)\;d^{3}r = 1, \tag{14}$$

We have determined the ground state energy of the hydrogenic impurity with three different methods: first, traditional variational method, second QGA with parameter optimization and QGA with wave function optimization.

3.1.1. Variational Method

The variational method is based on minimization of energy. Using the wave function defined in Eq. (13) an energy expectation value can be determined for each value of the variational parameter λ. The wave function with the λ value which minimizes the energy is accepted as the solution of the problem and the corresponding energy is accepted as the ground state energy. It is clear that this method is limited to the wave function space determined by the analytical form given in Eq. (13).

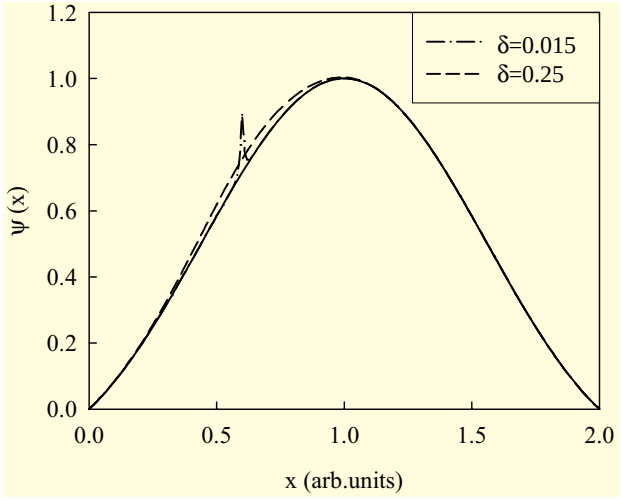

Figure 8. The effect of the mutation width, δ, on the wave function.

3.1.2. Quantum Genetic Algorithm method

The QGA method described above is also based on the minimization of energy. In this study we have used two different forms of QGA. The first form is based on parameter optimization, and the second one on the wave function optimization. Both forms have some common properties.

In the first step, one creates an initial population of possible solutions of the problem. For this purpose, random values of the parameter λ are chosen for each individual in the population. Then each individual in this initial population is normalized by Eq. (14) and the energy expectation value is calculated from the relation

$$E_i =< \phi_i^* | \hat{H} | \phi_i >, \qquad i = 1, 2, ..., N_{pop} \tag{15}$$

In this study, we have chosen N_{pop}=100. The fitness values are evaluated from Eq. (4) using these energy expectation values. Then the copying operation is performed on the population.

3.1.3. QGA with Parameter Optimization

In this approach, the individuals are represented by the variational parameter λ, and the binary code of this parameter is used as the genetic code. Following the application of copying operation, the crossover and mutation operations are performed on this parameter as described above for parameter optimization. Crossover and mutation operations are separately performed with a predefined probability, therefore some individuals are subjected to both operations, while some individuals are subjected to just one operation or no operations all. We show a sample crossover operation in the following

$$\lambda_1 : 10101\mathbf{111} = 0.68359375 \qquad \lambda_1' : 10101\mathbf{010} = 0.66406250,$$

$$\lambda_2 : 10010\mathbf{010} = 0.57031250 \qquad \lambda_2' : 10010\mathbf{111} = 0.58984375,$$

here two new individuals, λ_1', λ_2', are derived from two existing individuals λ_1, λ_2 . Also a mutation operation is shown below

$$\lambda_1 : 101\mathbf{0}1111 = 0.68359375 \qquad \lambda_1' : 101\mathbf{1}1111 = 0.74609375.$$

After these genetic operations, a new population is obtained and this new population is again normalized. Of course this approach also cannot change the analytical form of the trial wave function it can only numerically determine the best λ value.

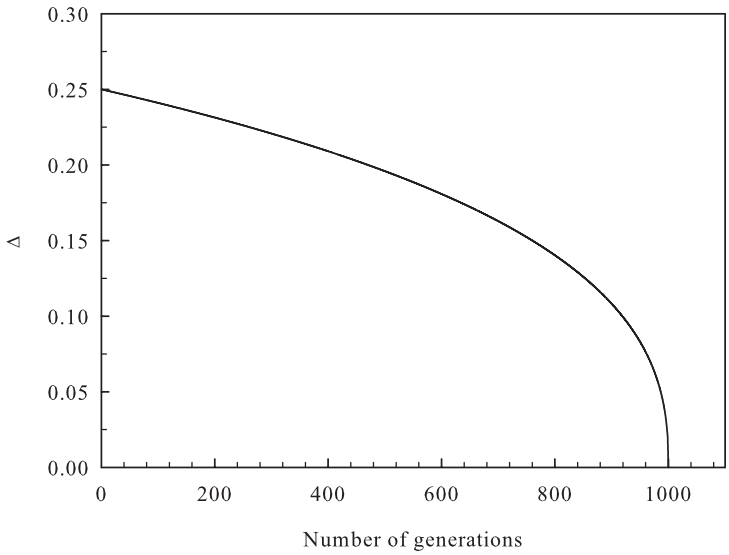

Figure 9. Variation of the mutation intensity with the generations.

3.1.4. QGA Based on Wave Function Optimization

In this approach, the wave function itself is considered as the genetic code representing the individual, instead of the parameter λ in Eq. (13). The main difference here is that the wave function is discretized on a space mesh with equal intervals of h. There are n mesh points and the wave function of the individual is represented by n values corresponding to these mesh points. Therefore, the wave functions of all the individuals in the population are represented by an array $\phi_{i,j}$ $(i = 1...N_{pop}, j = 1...n)$. This population is normalized according to Eq. (14) with numerical integration. Expectation values of total energy are determined for each individual. These energy values are used to determine the fitness values and to apply the copying process as described above in Section 2.

The crossover and mutation operations are applied randomly to these individuals with a predetermined probability. In this study, we have chosen the probability of crossover as 0.95 and probability of mutation 0.05. The crossover and mutation operations are performed numerically at each mesh point employing Eqs. (5),(6) and Eqs. (7), (8) respectively. The amplitude of the mutations is decreased according to Eq. (9). The new generation is normalized after all these genetic operations.

In this study, we have not considered any specific material therefore we have used the numerical constants representing hydrogen atom, i.e. effective Bohr radius a_0=0.529 Å, and effective Rydberg energy R_y=13.6 eV.

3.2. Results and Discussion

The results obtained from the calculations are presented comparatively in Table 1 along with the exact results. The first column in Table 1 corresponds to the radius of the well, i.e. the confining potential, other columns are the energies obtained from (a) exact calculation [38, 39], (b) variational calculation [38], (c) QGA based on parameter optimization and (d) QGA based on wave function optimization.

As can be seen from the table total energy of the electron in its ground state are positive for small confining radii, this means that dominant influence on the motion of the electron is due to the walls and therefore the electron has a very high kinetic energy. In this case electron does not feel the effect of the impurity. However as the radius increase, the influence of the confining walls diminishes and the motion of the electron is dominated by the impurity, the electron becomes bounded to the impurity when the radius is

Table 1. Ground state energies of a hydrogenic impurity in spherical quantum dot of infinite depth with a radius (R). (a) exact calculation [38, 39] (b) variational calculation [38], (c) QGA based on parameter optimization and (d) QGA based on wave function optimization.

R (a_0)	**Energy**^{a}	**Energy**^{b}	**Energy**^{c}	**Energy**^{d}
0.5	29.4959	29.5241	29.5241	29.4984
1.0	4.7480	4.7768	4.7767	4.7517
1.2	2.5386	2.5675	2.5674	2.5401
1.6	0.5426	0.5715	0.5714	0.5445
1.8	0.0651	0.0938	0.0938	0.0662
2.0	-0.2500	-0.2216	-0.2216	-0.2489
2.4	-0.6128	-0.5854	-0.5854	-0.6116
2.8	-0.7933	-0.7675	-0.7676	-0.7915
3.0	-0.8479	-0.8231	-0.8231	-0.8446
3.2	-0.8878	-0.8641	-0.8640	-0.8855
3.6	-0.9387	-0.9175	-0.9175	-0.9361
3.8	-0.9547	-0.9349	-0.9348	-0.9540
4.0	-0.9665	-0.9481	-0.9481	-0.9641
5.0	-0.9928	-0.9811	-0.9811	-0.9922
6.0	-0.9985	-0.9918	-0.9917	-0.9966
7.0	-0.9997	-0.9958	-0.9958	-0.9992

approximately equal to $2.0a_0$. As the radius is increased further the energy of the ground state approaches to that of free hydrogen i.e. –1.0 Rydberg, indicating that the electron does not feel the potential wall. These qualitative results are the same for all of the methods.

The results of the variational method and the QGA based on parameter optimization are very close to each other. In this case, especially when there is only one variational parameter, employing the QGA has no advantage at all, and it just makes the solution more complex. However, the QGA based on wave function optimization produce results very close to the exact ones, and the results significantly differ from the variational method. This demonstrates the power of the QGA and its superiority over traditional variational method. Also, one may conclude that the choice of the genetic code representing the individual is extremely important in QGA applications.

Figures 10 and 11 show the wave functions obtained from variational method and the QGA with wave function optimization for $R = 1.0a_0$ and $R = 7.0a_0$ respectively. There is a significant difference between the two wave functions, especially near the center of the dot. The analytical form of the wave function in the variational method is restricted, whereas there is no restriction on the form of the wave function in QGA with the wave function optimization. The value of the wave function can be adjusted at each mesh point as needed. This flexibility constitutes the basis for the superiority of the QGA method.

The convergence time of the QGA depends, generally, on the complexity of the problem under consideration. However, as seen from Figure 12, 15 to 20 generations are sufficient for the convergence of the solution to the problem considered here, and these results were repeatable with different initial populations.

3.3. Self-consistent electronic structure calculation of semiconductor heterojunction

In this application of GA, we have investigated the ground state energy level of electrons in modulation doped GaAs/$Al_xGa_{1-x}As$ heterojunctions. For this purpose, Schrödinger and Poisson equations are solved self consistently using quantum genetic algorithm (QGA). Thus, we have found the potential profile, the ground state subband energy and their corresponding envelope functions. Other properties of this structure were presented in Ref. [11, 30].

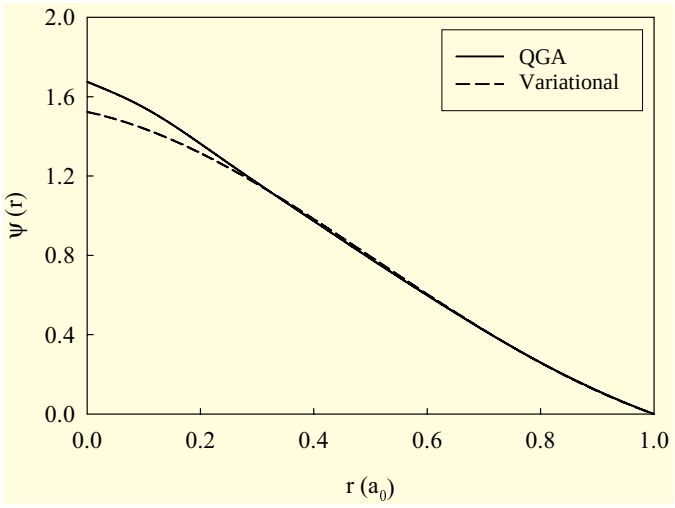

Figure 10. Wave function obtained from both variational and genetic algorithm for $R_{dot} = 1.0a_0$.

The two-dimensional electron gas (2DEG) of a modulation-doped GaAs/$Ga_{1-x}Al_xAs$ heterostructure is readily formed in electronic devices such as high electron mobility transistor (HEMT) and quantum well infrared photodetector (QWIP) [3, 39–42]. Studies of the energy levels, electron mobility, optical and other physical properties of 2DEG using analytical and numerical approaches have been reported in numerous studies [43–50].

As well known, to determine the energy levels and charge transfer in a single heterojunction, coupled Poisson and Schrödinger equations have to be solved with self-consistently,

$$\left[-\frac{\hbar^2}{2}\frac{\partial}{\partial z}\frac{1}{m(z)}\frac{\partial}{\partial z} + V_b(z) - eV_H(z)\right]\psi_i(z) = E_i\psi_i(z), \tag{16}$$

$$\frac{d^2V_H(z)}{dz^2} = \frac{4\pi e}{\kappa(z)}\left[\sum_i n_i\psi_i^2(z) - N_D^+ + N_A^-\right], \tag{17}$$

where $V_H(z)$ is the Hartree potential, $V_b(z)$ is the barrier potential, n_i is the areal concentration of electrons in the ith subband, N_D^+ and N_A^- are the ionized donor and acceptor concentration respectively, κ(z) and $m(z)$ are the position-dependent static dielectric constant and effective mass respectively.

The Schrödinger equation is solved by GA method and the Hartree potential arising from electron-electron interaction is calculated from Eq. (17) by finite difference iteration method [11].

At finite temperature T, the chemical potential of the electrons μ and the quantities n_i, E_i, m_i are related by:

$$n_i = m_i\frac{k_BT}{\pi\hbar^2}\ln\left[1 + \exp\left(\frac{\mu - E_i}{k_BT}\right)\right], \tag{18}$$

where k_B is the Boltzmann constant. At $T = 0$ K, this equation reduces to

$$n_i = \frac{m_i}{\pi\hbar^2}\left(\mu - E_i\right)\Theta\left(\mu - E_i\right), \tag{19}$$

where Θ is the step function. The above set of equations needs to be completed by boundary conditions. The bound state envelope function $\psi_i(z)$ should go to zero while $z \to \pm\infty$ and $\frac{1}{m(z)}\frac{\partial\psi_i}{\partial z}$ should be continuous everywhere. As for the Poisson equation, it is required that the heterojunction be in electrical equilibrium, namely

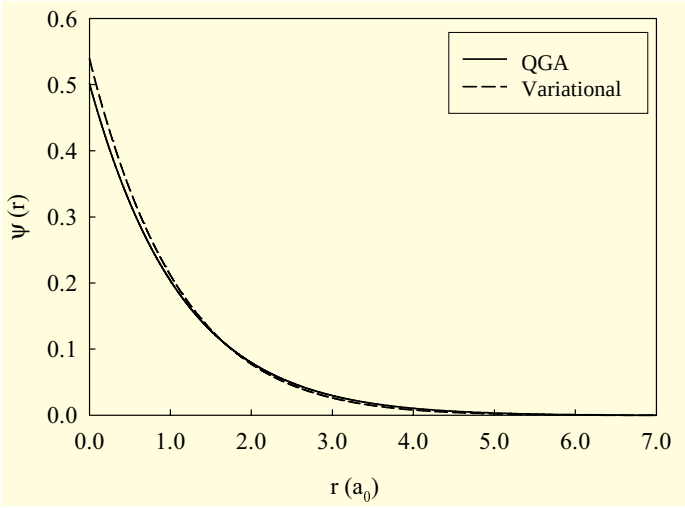

Figure 11. Same as Figure 10 but for $R_{dot} = 7.0a_0$.

$$\sum_i n_i + \int_{-\infty}^{\infty} \left(N_A^-(z) - N_D^+(z) \right) dz = 0. \tag{20}$$

In addition, the heterojunction is in thermodynamical equilibrium. This condition requires the chemical potential to be constant in the both regions. The full formulation of this problem is found in Ref. [11, 30, 51, 52].

In this study, we have used modified Fang-Howard [47, 51] trial wave function, which allows penetration into the barrier region and obeys the boundary condition mentioned in section 2. This wave function is

$$\psi_k(z) = \begin{cases} A \exp(\alpha_k z/2) & z \leq 0 \\ B(z+z0) \exp(-\beta_k z/2) & z \geq 0 \end{cases}, \tag{21}$$

with random values for $\alpha_k > 0$ and $\beta_k > 0$. A and B are normalization constants and they determined numerically by means of

$$\int_{-\infty}^{\infty} \psi_k^*(z)\psi_k(z)dz = 1. \tag{22}$$

We have chosen population number (*npop*) as 100. A normalized random population of wave functions (individuals) is created for random values of α_k and β_k ($k = 1 \ldots npop$) using Eqs. (21), and (22) and assigned to two dimensional vector arrays as an initial generation. Expectation value of energy is determined from this generation by means of Eq. (15). Fitness values are created using these energy values by Eq. (4).

The crossover operation is performed numerically at each mesh point employing Eq. (5). *St* in Eq. (5) is a smooth step function (i.e. Eq.(6)) or its value can be randomly selected from a uniform distribution between (0,1). At each step of GA iteration, type of crossover process(namely the selection of the smooth step function or a random real number) is randomly determined. In this problem, we have seen that this crossover scheme is more efficient and the probability of both crossover types has been chosen as 0.50.

In mutation operation, random values were assigned to α and β parameters in Eq. (21). In this way, a $\psi_M(z)$ mutation function was constructed and function was added to another randomly chosen $\psi_k(z)$ function to create a new parent function as

$$\psi_k'(z) = \psi_k(z) + C\psi_M(z), \tag{23}$$

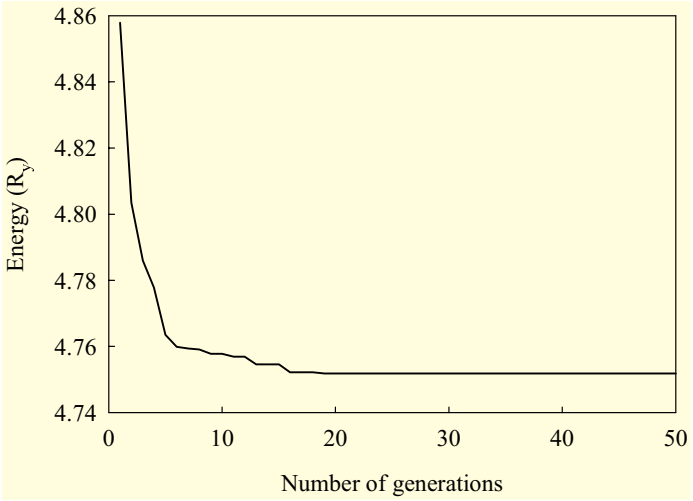

Figure 12. Evolution of energy eigenvalue of donor impurity for $R_{dot} = 1.0a_0$.

where C is the amplitude of mutation function.

During all of the GA iteration, copy or reproduction, crossover and mutation operations were randomly performed over the individuals. After the application of the genetic operations, obtained new populations were normalized.

Our algorithm may be summarized briefly as follows:

- *i*) Firstly, initial population is created and normalized.
- *ii*) The expectation values of energy are determined for each individual in the barrier potential. Hartree potential initially is taken as zero.
- *iii*) Fitness values are computed with these energy eigenvalues and the best fitness determined.
- *iv*) A new generation is created from old one with genetic operations (copy or reproduction, crossover and mutation operations) and then normalized.
- *v*) Poisson's equation is solved using the wave function which corresponds to the best fitness
- *vi*) Hartree potential calculated is added to the barrier potential and returned back to step *ii*.

This process is repeated until sufficient convergence is obtained.

3.3.1. Results and Discussion

The parameters used in this study are listed in Ref. [11]. In Figure 13, the calculated self-consistent Hartree potential V_H, ground state subband energy and Fermi energy level are shown. In the inset, tunneling electron concentrations N_s determined self-consistently is shown. In this calculation, the exchange and correlation energies are not considered. Also the ground state subband wave function, which is determined by QGA, is given in this figure.

In Figure 14, the evolution of energy eigenvalue with the number of iterations is plotted. As seen from this figure, the variation of the energy eigenvalue with iteration shows initially an oscillatory behavior, then it converges to a constant value after nearly 60 iterations. The reason for this oscillation is the fact that the best fitness is not carried to the new generation because of the self-consistent procedure.

Figure 15 shows the evolution of the concentration of 2DEG versus the number of iterations. Here the oscillatory behavior is similar to Figure 14. These oscillations are due to the electrical and thermodynamical

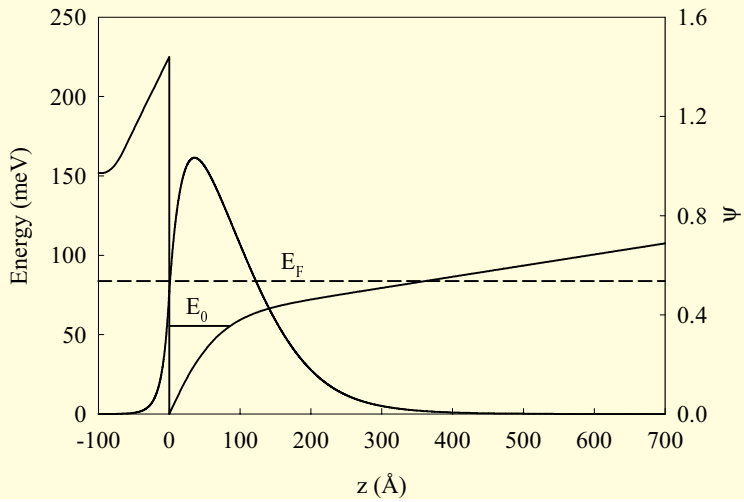

Figure 13. The calculated self-consistent potential, the ground subband, Fermi energy and envelope function.

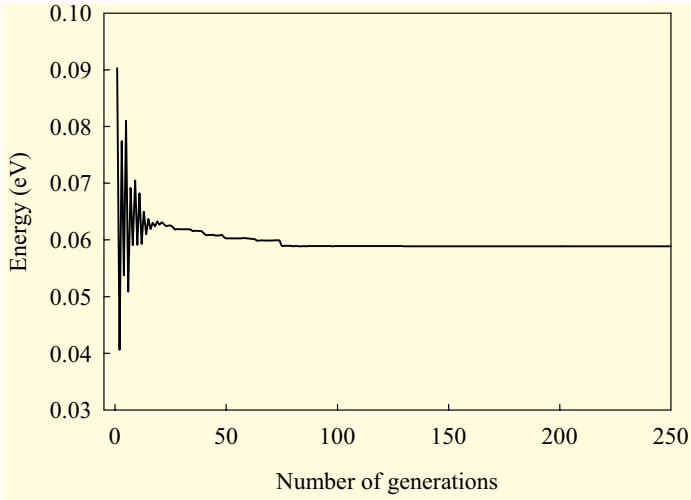

Figure 14. The evolution of the energy eigenvalue with the generations.

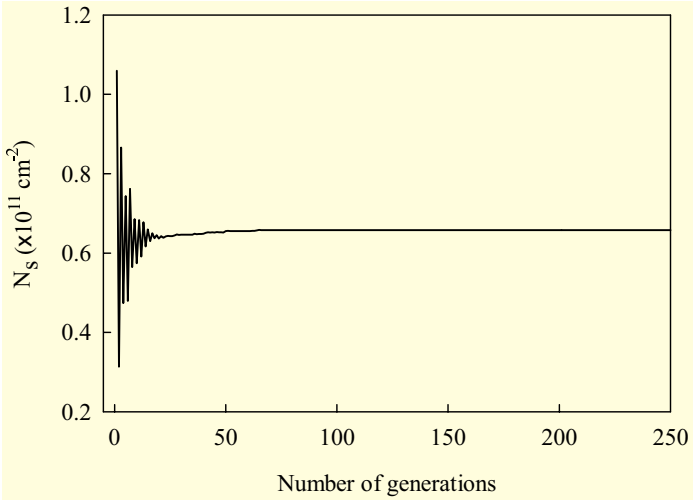

Figure 15. The evolution of 2DEG concentration with the generations.

nonequilibrium. After some 50 iterations, system reaches to the electrical equilibria and the oscillations vanish.

All results are in agreement with the literature [51, 52]. As shown in the results, QGA method is quite efficient for the self-consistent heterojunction problem. So, this method can be applied to the calculation of the electronic structure of quantum nanostructures.

3.4. Self-consistent electronic structure calculations of a quantum dot with many electrons

In this application of GA, we have calculated energy levels of an N-electron quantum dot. Simultaneous solutions of the coupled Schrödinger and Poisson equation have been realized by GA in the Hartree approximation and the results obtained were compared with the matrix diagonalization ones. We have determined some physical properties of the system taken into consideration such as single particle energy levels, total energy, etc. Also the applicability of QGA to many-electron quantum systems was checked and evaluated its effectiveness [13, 30].

In this study, we have considered a spherically symmetric quantum dot (QD), where the dot consists of GaAs and the surrounding bulk matter consists of AlGaAs. The difference between the band gaps of these semiconductor materials forms a confining potential, V_0, for the electrons inside the dot.

Schrödinger's equation for N interacting electrons confined in such a potential is

$$\hat{H}\psi\left(r_1, r_2, .., r_N\right) = E\psi\left(r_1, r_2, .., r_N\right) \tag{24}$$

For the system under consideration, we can write the N-particle Hamiltonian in the effective mass approximation as

$$\hat{H} = \sum_{i=1}^{N} -\frac{\hbar^2}{2}\vec{\nabla}\left(\frac{1}{m^*}\vec{\nabla}\right) + \frac{1}{2}\sum_{i=1}^{N}\sum_{\substack{j=1 \\ i\neq j}}^{N}\frac{1}{\varepsilon\left|\vec{r}_i - \vec{r}_j\right|} + V_0, \tag{25}$$

where ε is the relative dielectric coefficient. For a spherically symmetrical confining potential $V_0(r)$, single particle Schrödinger equation for our system in the Hartree approach

$$\left[-\frac{\hbar^2}{2}\vec{\nabla}\left(\frac{1}{m^*\left(r\right)}\right)\vec{\nabla} + \frac{\ell\left(\ell+1\right)\hbar^2}{2m^*\left(r\right)r^2} + V_0\left(r\right) - eV_H\left(r\right)\right]R_i\left(r\right) = \varepsilon_i R_i\left(r\right) \tag{26}$$

where $\hbar$ is reduced Planck's constant, $m^*(r)$ is effective mass, ℓ is angular momentum quantum number, $V_0(r)$ is the confining potential, e is the electron charge. $V_H(r)$ is the Coulomb potential due to the electron-electron interaction and is determined from the Poisson equation

$$\left(\frac{d^2}{dr^2}+\frac{2}{r}\frac{d}{dr}\right)V_H\left(r\right)=\frac{4\pi e}{\varepsilon\left(r\right)}n\left(r\right) \tag{27}$$

where $\varepsilon(r)$ is the dielectric coefficient depending on the position and $n(r)$ is the charge density. The charge density inside the QD is,

$$n\left(r\right)=-\sum_{i=1}^{N}\left|\psi_i\right|^2. \tag{28}$$

Noting that $\psi_i = R_i(r)Y_{\ell m}(\theta,\varphi)$, we have $|\psi_i|^2 = |R_i|^2 Y^*_{\ell m}(\theta,\varphi)Y_{\ell m}(\theta,\varphi)$. The spherical harmonics are normalized and have the property [53],

$$\sum_{m=-\ell}^{\ell}Y^*_{\ell m}\left(\theta,\varphi\right)Y_{\ell m}\left(\theta,\varphi\right)=\frac{2\left(2\ell+1\right)}{4\pi}. \tag{29}$$

Details of the distribution of the charge to the atomic shells were explained in Ref. [30, 13].

In order to determine the single particle energy levels Eqs. (26), (27) and (28) should be solved self-consistently. The electrons move in an electric field, however, this electric field depends on the charge density and this in turn is determined by the wave function itself. Consequently, the solution of the Schrödinger equation must be consistent with the potential field induced by its own charge distribution.

In this application of the method wave functions are considered as the individuals on which the genetic operations are to be applied. Although the initial population is not very important having a good initial population may speed up the convergence. Therefore, considering the penetration into the barrier region, initial population is formed from the Gaussian like functions

$$R_{k,\ell}(r)=A_k r^{\ell}\exp\left(-\alpha_k r^{M_k}\right), \tag{30}$$

where, the index k points to the individual in the population ($k=1\ldots n_{pop}$), A_k is the normalization factor of the individual, ℓ is the orbital angular momentum quantum number, α_k is a random number between $(0, R_{max})$ and M_k is an integer between 2 and 4.

The normalization factor A_k is determined numerically from the normalization condition

$$\int_0^{R_{\max}}\left|R_{k,\ell}\left(r\right)\right|^2 r^2 dr=1. \tag{31}$$

The initial population is generated from Eq. (30) for random values of α_k and M_k. Population number is chosen as n_{pop}=100. Each individual consists of two such wave functions, one for the s-shell with ℓ=0 and another one for the p-shell with ℓ=1. This population is stored in a four dimensional array and normalized according to Eq. (31). Thus, we have obtained a pool of probable solutions to the problem. Single particle energies are determined from

$$\varepsilon_{k,\ell}=\left\langle R_{k,\ell}\left(r\right)\left|\hat{H}\right|R_{k,\ell}\left(r\right)\right\rangle \tag{32}$$

for each individual (or the wave function pair) in this pool.

Using the single particle energies of each individual, the total energy of the system is determined for each individual, i.e.

$$E_k=\sum\varepsilon_{k,\ell}-\frac{1}{2}\int R^*_{k,\ell}\left(r\right)V_H\left(r\right)R_{k,\ell}\left(r\right)r^2dr. \tag{33}$$

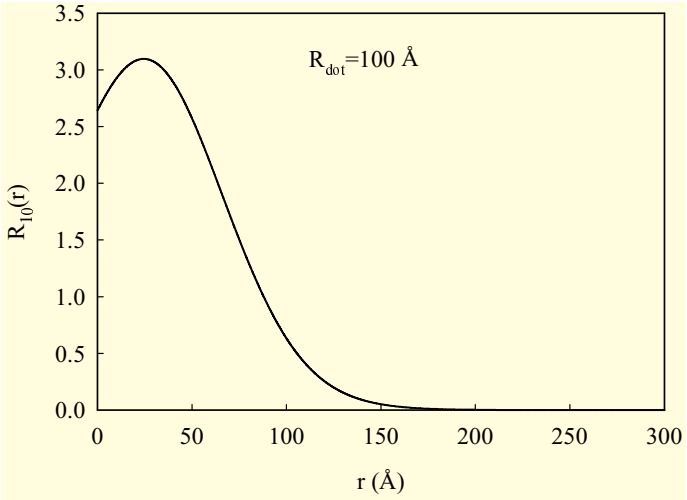

Figure 16. Effect of the smooth step crossover on the wave function.

The aim of QGA is to minimize this total energy. For this purpose, standard genetic processes explained above are used. Fitness values were produced using the total energy in the Eq. (4). Using these fitness values as probabilities a new generation is formed from randomly chosen individuals with the copy operation.

In the crossover operation, the expression defined in Eq. (5) was employed using random number chosen uniformly from the interval (0,1) for St. In this problem, if the smooth step function is used for the St, a falling down is to be on the wave function as seen in Figure 16.

In the mutation, an individual is chosen from the current generation, then this is changed as

$$R'_{1,\ell} = R_{1,\ell} + \Delta B R_M(r) \tag{34}$$

where B is a random number in the interval (0,1), Δ is the mutation intensity and it changes from generation to generation as explained in section 2.3, Eq. (8). We have chosen d=0.4 in Eq. (8). $R_M(r)$ of Eq. (34) is the mutation function, and the expression in Eq. (30) is used for $R_M(r)$.

All genetic operations (copy, crossover and mutation) are performed randomly and the new generation, obtained by application of these genetic operations, is normalized.

Derivatives are evaluated on a mesh with a 5-point method, and Simpson's method is utilized for integral evaluations. In order to determine the Hartree potential $V_H(r)$ electron density corresponding to the individual with the best fitness is used in Eqs. (27) and (28).

The algorithm can be summarized as follows:

- i) Generate an initial population and normalize each individual in this population.
- ii) Evaluate the single particle energies considering the confining potential V_0. In the first iteration step $V_H(r)$ is taken as zero.
- iii) Obtain total energy values for each individual and use these energy values to determine fitness values of each individual.
- iv) Find the best individuals
- v) New generation is created from the current generation through the genetic operations.
- vi) Wave functions of the best individual are used to determine the charge density inside the dot and Poisson's equation is solved to find Hartree potential $V_H(r)$.
- vii) Hartree potential is combined with the confining potential and go back to step ii.

This loop is continued until sufficiently good convergence is obtained.

3.4.1. Results and Discussion

The material parameters used in this problem are listed in Refs. [13, 30]. Simultaneous solution of coupled Poisson and Schrödinger equations were obtained with both matrix diagonalization (MD) and QGA. Figure 17 shows the total energy of the electron cloud inside the dot. Solid symbols correspond to the results obtained from QGA and open symbols correspond to the results of MD. Absolute value of the energy difference between the two methods is of the same order of magnitude, however as the total energy is much larger the relative magnitude of the difference gets smaller. As a result, in Figure 17 the symbols representing the results of the two methods completely overlap and the difference is almost indistinguishable.

Figure 18 shows the electron density inside the dot for various numbers of contained electrons for $R_{dot} = 1.0a_0^*$. It can be seen that the electrons penetrate into the barrier, and as expected this penetration increases as the number of electrons inside the dot increases. Again the solid and open symbols correspond to QGA and MD, respectively. It appears that there exists a considerable difference in electron densities between

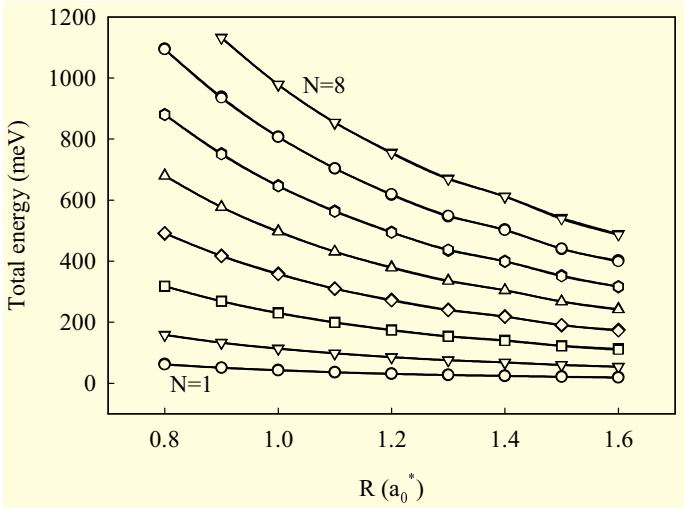

Figure 17. The total energy of the electron gas inside the dot.

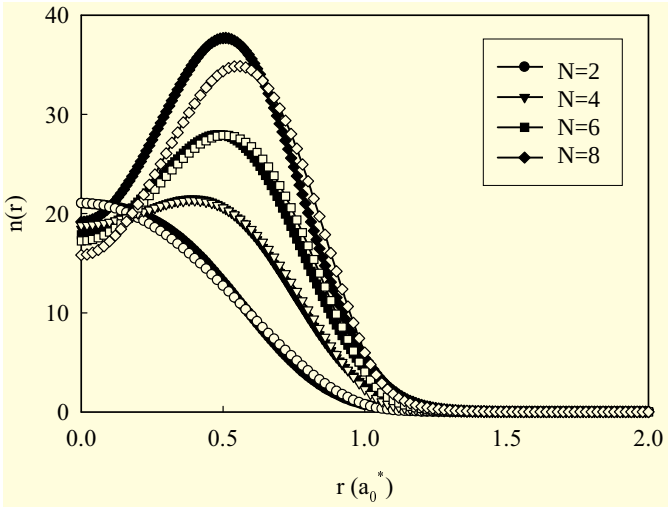

Figure 18. The electron density of electron gas inside the dot for $R_{dot} = 1.0a_0^*$.

the methods and this difference increases with the increasing number of electrons. However, this difference does not show itself on the single particle and total energies. QGA is based on the energy minimization, and this insensitivity of the energy to the changes in the electron density (or the shape of the wave functions) is the basic reason of the discrepancy in the electron density. This could be a major drawback for the QGA. Therefore it might be concluded that QGA is more appropriate when one is mainly interested in energy level structure. Also, in cases where the total energy significantly depends on the electron distribution (or the shape of the wave functions) QGA is expected to give better results for the electron distribution as well.

It is also interesting to compare the numerical efforts of the two methods. In QGA one only has to evaluate the fitnesses (energy expectation values) for each individual and this is accomplished by integration over the grid. If the grid has N mesh points, required numerical effort is proportional to N. MD is on the other hand requires evaluation of the eigenvalues and eigenvectors of an $N \times N$ matrix, and the numerical effort required for this operation is proportional to N^3. QGA may be relatively slower when the number of mesh points is smaller, however as the number of mesh points increases QGA becomes more favorable. The linear increase in the numerical effort makes QGA applicable on even a moderate PC to the cases with much larger number of mesh points. Especially, problems in more than one-dimension would require so many mesh points, and even for a two dimensional problem MD would require a large mainframe.

In Figure 19, we display the CPU times used by two methods. The CPU times are obtained on a PC with a PIII-667 MHz CPU and 128 MB of RAM. In most cases, sufficient convergence obtained after a few hundred generations of QGA. Therefore, CPU times for 500 and 1000 generations are displayed in Figure 19. On the other hand, MD method has converged after 15-20 iterations, so we have displayed the CPU times for 20 iterations. It can be clearly seen in Figure 19 that the numerical effort of QGA linearly and that of MD cubically depends on the number of mesh points.

It is important to address the effects of the number of generations and the number of individuals in the population. We have taken a five-electron dot as a sample case. We have repeated the calculations with 25 different seeds for the random number generator for n_{pop}=50, 100 and 150. In Figure 20(a), variation of the total energy (averaged over 25 different seeds) with number of generations is shown. As expected, n_{pop}=50 has a slower convergence, however n_{pop}=100 and n_{pop}=150 have similar convergence behavior. The diversity and chances for the existence of a good individual increase as the number of individuals in the population increases. However, this increase in the variety saturates at a sufficiently large n_{pop}, and by increasing n_{pop} beyond this point we do not gain much.

One may conclude by comparing the cases for n_{pop}=100 and n_{pop}=150 in Figure 20(a) that the case with larger n_{pop} converges faster. This is true in terms of the number of generations. However, what really matters is the total computational effort needed to obtain a sufficient convergence. Here, the computational

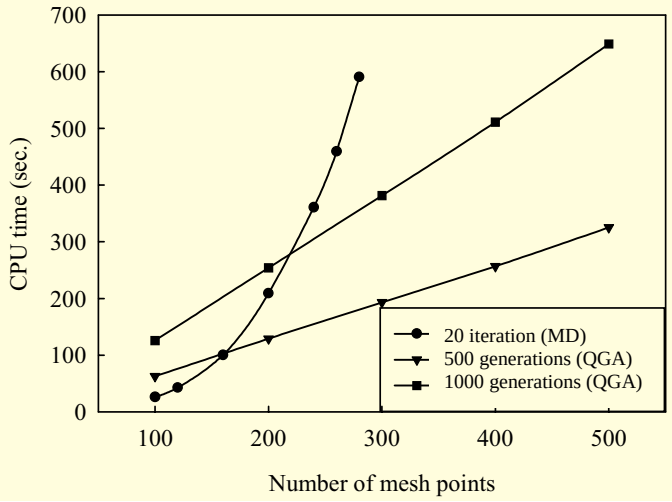

Figure 19. Comparison of CPU times required for different number of mesh points.

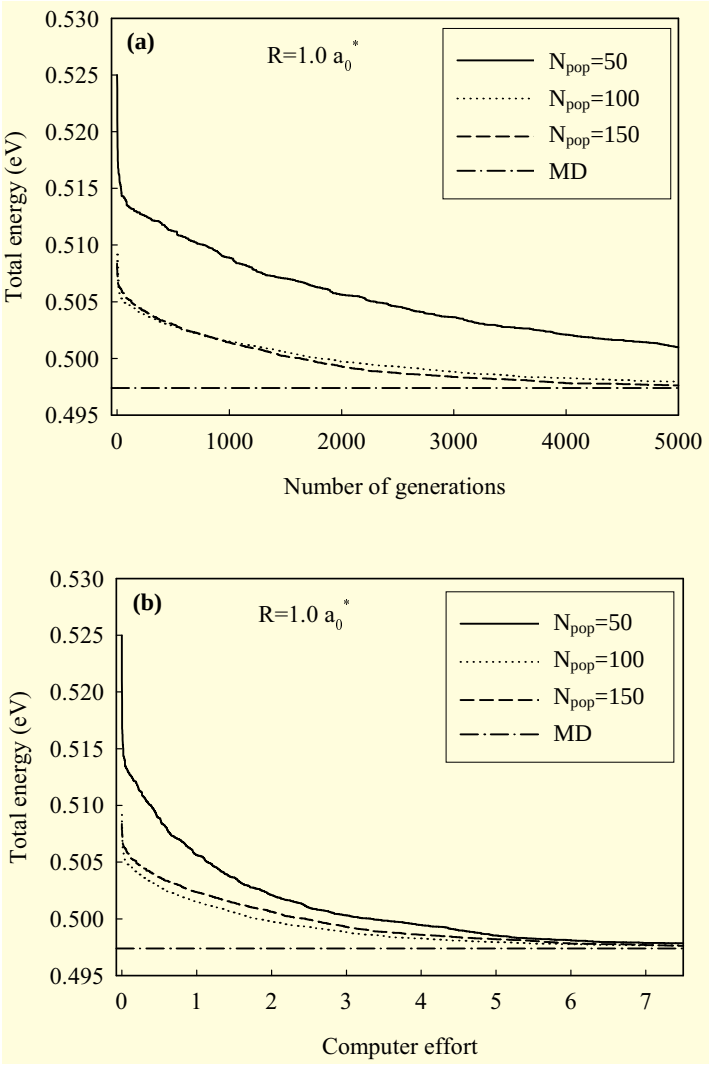

Figure 20. a) Evolution of total energy for a five-electron quantum dot with number of generations for different population sizes. (b) Evolution of total energy for a five-electron quantum dot with computational effort for different population sizes.

effort is proportional to n_{pop} times the number of generations. We show the average value of the total energy against the computational effort in Figure 20(b) where it can be seen that all cases with n_{pop}=50, 100 and 150 have similar convergence behavior. We see that their convergence rates for the cases for n_{pop}=100 and n_{pop}=150 are almost the same and the differences between them can be accounted for in terms of the effects of the initial population. Thus, in terms of total computational effort increasing the population size does not contribute much to the acceleration of the convergence.

As a result, increasing the population size beyond some value contributes neither to the diversity in the initial population nor to the acceleration of the convergence. One should therefore use a sufficiently large population to enhance the diversity in the initial population however increasing the population beyond some saturation value does not contribute much to the efficiency of the QGA. For the problem considered in this study n_{pop}=100 would be an appropriate choice.

4. Conclusion

We have calculated the electronic structure of three different structures, hydrogenic donor impurity in a spherical quantum dot, modulation doped heterojunction and a many-electron spherical quantum dot. In the self-consistent calculation, second and third problems, we have formulated the problem under the Hartree approximation. In the calculations, we use quantum variational method, genetic algorithm and matrix diagonalization techniques and solve the Poisson and Schrödinger equations self-consistently. All of the results indicate that the QGA is quite efficient for the analysis of realistic self-consistent or non-self-consistent quantum mechanical problems.

In addition, extension of the QGA method to 2-dimensional systems is not very hard [20] and can easily be implemented on even a small PC. Therefore, it seems that QGA may be a powerful alternative to other methods currently used for the analysis of self-consistent quantum mechanical problems.

Acknowledgments

This study is a part of the Ph.D. Thesis of one of the authors (M. Şahin) and was partially supported by Selçuk University under grant no: BAP2001/112.

References

[1] L. Banyai, S. W. Koch, *Semiconductor Quantum Dots*, Singapore, (World Scientific, Singapore, 1993).

[2] D. Bimberg, M. Grundmann, N. N. Ledentsov, *Quantum dot heterostructures*, (John Wiley&Sons, Chichester, 1999).

[3] B. F. Levine, *J. Appl. Phys.*, **74**, (1993), R1.

[4] V. Ryzhii, *Semicond. Sci. Technol.*, **11**, (1996), 759.

[5] S.-W. Lee, K. Hirakawa, Y. Shimada, *Physica E*, **7**, (2000), 499.

[6] J. I. Lee, H. G. Lee, E.-J. Shin, S. Yu, D. Kim, G. Ihm, *Appl. Phys. Lett.*, **70**, (1997), 2885.

[7] D. Jovanovic, J.-P. Leburton, *Phys. Rev. B*, **49**, (1994), 7474.

[8] M. Schreiber, J. Siewert, T. Vojta, *Int. J. Mod. Phys. B*, **15**, (2001), 3641.

[9] J. Sanchez-Dehesa, F. Aristone, G. Marques, *J. Phys. Soc. Jpn.*, **69**, (2000), 3904.

[10] S. Sinha, *Physica E*, **8**, (2000), 24.

[11] M. Şahin, M. Tomak, *Int. J. Mod. Phys. B*, **26**, (2002), 3883.

[12] M. Şahin, M. Tomak, *Physica E*, **28**, (2005), 247.

[13] M. Şahin, Ü. Atav, M. Tomak, *Int. J. Mod. Phys. C*, **16**, (2005), 1379.

[14] J. H. Holland, *Adaptation in Natural and Artifical Systems*, (University of Michigan Press, Michigan, 1975).

[15] A. Prügel-Bennett, J. L. Shapiro, *Physica D*, **104**, (1996), 75.

[16] E. S. Kim, C. Oh, S. Lee, B. Lee, I. Yun, *Microelectronics Journal*, **32**, (2001), 563.

[17] P. Chaudhury, S. P. Bhattacharyya, *Chem. Phys. Lett.*, **296**, (1998), 51.

[18] H. Nakanishi, M. Sugawara, *Chem. Phys. Lett.*, **327**, (2000), 429.

[19] I. Grigorenko, M. E. Garcia, *Physica A*, **284**, (2000), 131.

[20] I. Grigorenko, M. E. Garcia, *Physica A*, **291**, (2001), 439.

[21] I. Grigorenko, M. E. Garcia, *Physica A*, **313**, (2002), 463.

[22] M. Sugawara, *Comp. Phys. Comm.*, **140**, (2001), 366.

[23] N. Chakraborti, P.S. De, R. Prasad, *Materials Letters*, **55**, (2002), 20.

[24] Ö. Şahin, P. Sayan, A. N. Bulutcu, *J. Cryst. Growth*, **216**, (2000), 475.

[25] A. Brunetti, *Comp. Phys. Comm.*, **124**, (2000), 204.

[26] L. Liu, L. Zhao, Y. Mao, D. Yu, J. Xu, Y. Li, *Int. J. Mod. Phys. C*, **11**, (2000), 183.

[27] Ş. Erkoç, K. Leblebicioglu, and U. Halici, *Mater. Manuf. Proces.*, **18**,(2003), 329.

[28] R. Saha, P. Chaudhury, S. P. Bhattacharyya, *Phys. Lett. A*, **291**, (2001), 397.

[29] C. T. Hsiao, G. Chahine, and N. Gumerov, *J. Comp. Phys.*, **173**, (2001), 433.

[30] M. Şahin, PhD Thesis, Department of Physics, Selçuk University, Konya, Türkiye, 2005.

[31] H. Şafak, M. Şahin, B. Gülveren, M. Tomak, *Int. J. Mod. Phys. C*, **14**, (2003), 775.

[32] D. A. Coley, *An Introduction to Genetic Algorithms for Scientists and Engineers*, (World Scientific, Singapore, 2001).

[33] D. E. Goldberg, *Genetic Algorithms in Search, Optimization, and Machine Learning*, (Addison Wesley Longman, Reading, 1999).

[34] M. Mitchell, *An Introduction to Genetic Algorithms*, (MIT Press, Boston, 1998).

[35] Z. Michaelwicz, *Genetic Algorithms + Data Structure =Evolution Programs*, 3rd ed., (Springer-Verlag, Heidelberg, 1998).

[36] M. W. Gutowski, *Journal of Phys. A*, **27**, (1994), 7893.

[37] N. Porras-Montenegro, S.T. Perez-Merchancano, *Phys. Rev. B*, **46** (1992), 9780.

[38] J. L. Marin, S. A. Cruz, *Am. J. Phys.*, **59**, (1991), 931.

[39] Y.P. Varshni, *Physics Lett. A*, **252**, (1999), 248.

[40] L. Thibaudeau, P. Bois, J. Y. Duboz, *J. Appl. Phys.*, **79**, (1996), 446.

[41] H. C. Liu, *Semiconductors and Semimetals*, **62**, (2000), 129.

[42] H. Morkoç, R. Cingolani, B. Gil, *Solid-State Electronics*, **43**, (1999), 1909.

[43] F. Stern, *Phys. Rev. B*, **5**, (1972), 4891.

[44] T. Ando, *J. Phys. Soc. Jpn.*, **51**, (1982), 3893.

[45] G. Bastard, *Surf. Science*, **142**, (1984), 284.

[46] B. Vinter, *Appl. Phys. Lett.*, **44**, (1984), 307.

[47] F. F. Fang and W. E. Howard, *Phys. Rev. Lett.*, **16**, (1966), 797.

[48] B. Vinter, *Appl. Phys. Lett.*, **44**, (1984), 307.

[49] T. Ando, A.B. Fowler, F. Stern, *Rev. Mod. Phys.*, **54**, (1982), 437.

[50] S. Hiyamizu, *Semiconductors and Semimetals*, **30**, (1990), 53.

[51] G. Bastard, *Wave Mechanics Applied to Semiconductor Heterostructures*, (Les Editions de Physique, Paris, 1988).

[52] K. F. Ilaiwi, M. I. El-Kawni, and M. Tomak, *Superlattices and Microstructures*, **24**, (1998), 61.

[53] R. Liboff, *Introductory Quantum Mechanics*, New York, AddisonWesley, 1998.